Domain structures of ferroelectric thin film controlled by oxidizing atmosphere

D. C. Ma, Yue Zheng’ , Biao Wang’ , and C. H. Woo

Citation: Appl. Phys. Lett. **99**, 142908 (2011); doi: 10.1063/1.3646387
View online: http://dx.doi.org/10.1063/1.3646387
View Table of Contents: http://aip.scitation.org/toc/apl/99/14
Published by the American Institute of Physics

APPLIED PHYSICS LETTERS **99**, 142908 (2011)

Domain structures of ferroelectric thin film controlled by oxidizing atmosphere

D. C. Ma,[1,2] Yue Zheng,[1,2,a)] Biao Wang,[1,b)] and C. H. Woo[2]

[1]*State Key Laboratory of Optoelectronic Materials and Technologies/Institute of Optoelectronic and Functional Composite Materials, School of Physics and Engineering, Sun Yat-sen University, Guang Zhou 510275, China*

[2]*Department of Electronic and Information Engineering, The Hong Kong Polytechnic University, Hong Kong SAR, China*

(Received 2 March 2011; accepted 25 August 2011; published online 7 October 2011)

Evolutions of domain morphology in the ferroelectric thin film subjected to the oxidizing atmosphere were predicted by using the phase field simulations, which incorporate the long-range electrostatic interactions and ionic surface charges. Due to effect of the oxidizing atmosphere, it is found that the ionic surface charges carried by oxygen can effectively change the internal electric filed, control the polarization orientation, and drive the domain wall motion of the ferroelectric thin film. Domain structures were simulated and also reveal that domain morphology of the ferroelectric thin film can be adjusted from a multi-domain to a mono-domain with increasing of the ionic charge density. © *2011 American Institute of Physics*. [doi:10.1063/1.3646387]

Ferroelectric thin films (FTFs) have become preferred materials in a wide variety of field effect transistors, ferroelectric memories, photomechanical sensors, and so on.[1–3] When FTFs are epitaxially grown on substrate, the polarization has an exclusive component perpendicular to the film surface due to the in-plane compressive misfit strain.[4] Although such orientations are desired for applications, uncompensated surface charges, due to the discontinuity of the normal polarization at the film boundaries, result in a depolarizing field that suppresses the spontaneous polarization and phase transition temperature.[5] The surface charges of FTF can be compensated by two metallic electrodes with the short-circuit boundary conditions. Whereas, for bare ferroelectric surface, there are no charges to compensate the polarization bound charges, and 180° stripe domains will be formatted to minimize the free energy due to effect of the depolarization field.[6]

According to recent experiments and simulations, the surface compensation by ionic adsorption plays an important role in the polarization stability and switching when FTF is exposed to an ambient environment.[7–13] Recent investigations have shown that the polarization state of a FTF without a covering electrode layer is extremely sensitive to the environment. H_2, O_2, H_2O, CO, CO_2, etc. absorbed on the bare ferroelectric surface can effectively compensate the bound charge and cause a potential to switch polarization of the ferroelectric film.[8–12] For a FTF with applied chemical potential, varying the surface ionic charge density can also change the switch mechanism from nucleation to continuous.[13] If the external perturbation can be well controlled, the polarization and domain structures of FTF can be artificially tuned or even switched. Furthermore, ionic surface compensation from the chemical environment brings up possibilities for optimization of thin film chemical actuators, memory, and catalysts.

In this paper, we adopt the phase field model (PFM) to describe the evolution of the spontaneous polarization field in a FTF. Taking into account the chemical potential, long-range electrostatic interactions, elastic contribution, gradient terms and surface effects, the influence of the oxidizing atmosphere on the spontaneous polarizations, and domain structures in the ultrathin FTF have been generally investigated.

We consider our thermodynamic reference as a crystal of infinite extent absent an applied field. Let $\mathbf{P}$ be the spontaneous polarization field, which is the polarization from the permanent electric moment formed from spontaneous atomic displacements. Therefore, the electric displacement field $\mathbf{D}$ can be expressed in terms of the linear part $\mathbf{P^E}$ and nonlinear part $\mathbf{P}$ as[14–18] $\mathbf{D} = \varepsilon_0\mathbf{E} + \mathbf{P^E} + \mathbf{P} = \varepsilon_0\mathbf{E} + \chi_\mathbf{b}\mathbf{E} + \mathbf{P} = \boldsymbol{\varepsilon}_\mathbf{b}\mathbf{E} + \mathbf{P}$, where $\chi_\mathbf{b}$ and $\boldsymbol{\varepsilon}_\mathbf{b}$ are the background susceptibilities and dielectric constants of the background material, respectively.[14–21] Since the background material is the paraelectric phase, which is a cubic crystal structure, the background dielectric constants in three axis directions are the same, i.e., $\varepsilon_b = \varepsilon_{11b} = \varepsilon_{22b} = \varepsilon_{33b}$.

In our PFM, the local spontaneous polarization vector, $\mathbf{P}(\mathbf{x}) = [P_1, P_2, P_3]$, were taken as the order parameter of the free energy, where $\mathbf{x} = (x_1, x_2, x_3)$. The temporal evolution of the spontaneous polarization was simulated by

$$\frac{\partial \mathbf{P}(\mathbf{x}, t)}{\partial t} = -M\frac{\delta F}{\delta \mathbf{P}(\mathbf{x}, t)}, \qquad (1)$$

where M is a kinetic coefficient related to the domain wall mobility, t is time, F is the total free energy of the simulated system. $\delta F/\delta \mathbf{P}(\mathbf{x}, t)$ is the thermodynamic driving force of the spatial and temporal evolution of the simulated system.

In following simulations, considering effect of the ionic surface charge determined by the oxygen atmosphere on the spontaneous polarization and domain structures of a FTF, we can express the total free energy in Eq. (1) as $F = F_0 + F_{\text{bulk}} + F_{\text{grad}} + F_{\text{elas}} + F_{\text{dep}} + F_{\text{chem}} + F_{\text{surf}} = F_0 + \int\int\int_V [f_{\text{bulk}} + f_{\text{elas}} + f_{\text{grad}} + f_{\text{dep}} + f_{\text{chem}}]\mathrm{d}V + \int\int_S f_{\text{surf}}\mathrm{d}S$,

---

[a)] Permanent address: School of Physics and Engineering, Sun Yat-Sen University, GuangZhou, China. Electronic mail: zhengy35@mail.sysu.edu.cn.

[b)] Electronic mail: wangbiao@mail.sysu.edu.cn.

0003-6951/2011/99(14)/142908/3/$30.00

where F_0, $F_{\rm bulk}$, $F_{\rm grad}$, $F_{\rm elas}$, $F_{\rm dep}$, $F_{\rm chem}$, and $F_{\rm surf}$ are the polarization and stress-strain independent part of the free energy, bulk-free energy, gradient energy, elastic energy, depolarization energy, electric energy arising from the chemical environment, and surface energy, respectively. V and S are the volume and upper-lower surfaces of FTF.

In total free energy density, $f_{\rm bulk}$ is expressed by the Landau polynomial expansion in terms of the polarization components

$$\begin{aligned} f_{\rm bulk} = {} & \alpha_1(P_1^2+P_2^2+P_3^2)+\alpha_{11}(P_1^4+P_2^4+P_3^4) \\ & +\alpha_{12}(P_1^2P_2^2+P_2^2P_3^2+P_1^2P_3^2) \\ & +\alpha_{111}(P_1^6+P_2^6+P_3^6)+\alpha_{112}[P_1^4(P_2^2+P_3^2) \\ & +P_2^4(P_1^2+P_3^2)+P_3^4(P_1^2+P_2^2)]+\alpha_{123}P_1^2P_2^2P_3^2, \end{aligned} \tag{2}$$

where $\alpha_1=(T-T_0)/2\varepsilon_0C_0$ is the dielectric stiffness, C_0 and T_0 are the Curie constants and Curie-Weiss temperature of the reference crystals, respectively. α_{11}, α_{12}, α_{111}, α_{112}, α_{123} are higher order dielectric stiffness coefficients.

The gradient energy density $f_{\rm grad}$ can be calculated through the gradients of the polarization field as $f_{\rm grad}=\frac{1}{2}G_{ijkl}P_{i,j}P_{k,l}$, where $P_{i,j}=\partial P_i/\partial x_j$, G_{ijkl} are the gradient energy coefficients (i, j, k, $l=1$, 2, 3).[4,6,14] The elastic energy density $f_{\rm elas}$ is generated from the phase transition and substrate constraint and can be expressed generally by $f_{\rm elas}=\frac{1}{2}c_{ijkl}(\varepsilon_{ij}-\varepsilon_{ij}^0)(\varepsilon_{kl}-\varepsilon_{kl}^0)$, where c_{ijkl} is the elastic stiffness tensor, ε_{ij} and ε_{ij}^0 are the total strain and eigenstrain, respectively. The eigenstrain connected with the ferroelectric transition is $\varepsilon_{ij}^0=Q_{ijkl}P_kP_l$, in which Q_{ijkl} represents the electrostrictive coefficient.[4] In addition, the total electric field is produced by the spontaneous polarizations and ionic surface charges from the chemical environment. If the electric field is only induced by the spontaneous polarizations, the electrostatic energy density is calculated from $f_{\rm dep}=-E_{{\rm d}i}\cdot P_i/2$, where $E_{{\rm d}i}$ is the depolarization field.[4,14] If oxygen adsorbed in bare surface of FTF, the electric energy arising from chemical environment can be written as $f_{\rm chem}=-E_{{\rm c}i}P_i$, where $E_{{\rm c}i}$ is the electric field induced by the surface ionic charges. The total electric field E_i is calculated by $E_i=E_{{\rm d}i}+E_{{\rm c}i}=-\phi_{,i}$. Suppose free charge inside the FTF does not exist, the electric displacement D_i satisfies the electrostatic equilibrium equation $D_{i,i}=0$. For an open-circuit electric condition without the surface ionic charges, $D_in_i=0$ on the top and bottom surfaces of the film, where n_i denotes the component of unit vector normal to the surfaces. When the surface ionic charges are taken into account, the electric field E_i can be solved from $D_{i,i}=0$ with the boundary condition $D_in_i=\rho$, in which ρ is the surface ionic charge density. The surface energy density $f_{\rm surf}$ can be characterized as a function of the effective extrapolation length δ^{eff}, i.e., $f_{\rm surf}=\frac{1}{2}(D_{11}P_3^2/\delta^{eff}+D_{44}P_1^2/\delta^{eff}+D_{44}P_2^2/\delta^{eff})$, where D_{11} and D_{44} are material coefficients relating to the gradient energy coefficients.

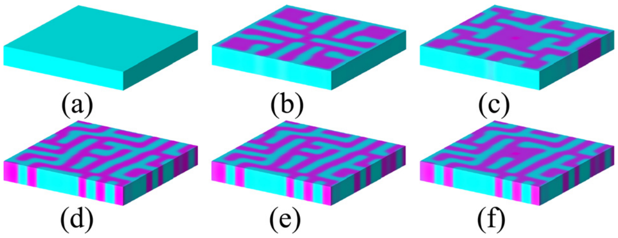

FIG. 2. (Color online) Steady domain morphologies of mono-domain with the present of (a) zero, (b) one, and (c) nine oxygen atom(s) on the center of the top surface; multi-domain with the present of (d) zero, (e) one, and (f) nine oxygen atom(s) on the center of the top surface. The (0, 0, P_3) and (0, 0, $-P_3$) domain are shown by magenta and cyan, respectively.

In the simulations, we employed $64\times64\times10$ discrete grid points at a scale of $\Delta x_1=\Delta x_2=1$ nm and $\Delta x_3=0.5$ nm to model an epitaxial $\rm PbTiO_3$ (PT) FTF with $\rm SrRuO_3$ bottom electrodes coherently strained to $\rm SrTiO_3$ substrate. The upper surface of the PT thin film was exposed to a controlled environment. Periodic boundary conditions were employed along the x_1 and x_2 directions. The material constants of the bulk-free energy were listed in Ref. 23, which were taken from Refs. 6, 22 and 24. As an example, the oxygen atmosphere was used to simulate the chemical environment and absorbed in the bare surface of the PT film along x_3-direction as shown in Fig. 1.

In a FTF with the open-circuit boundary condition, there is no charge compensation on the surface as shown in the left of Fig. 1. Based on PFM, we obtain the stable origin mono- and multi-domain structures at room temperature, which are shown in Figs. 2(a) and 2(d), respectively. Previous works[8,9] have suggested that negative ions bonded to the surface such as $\rm O^{2-}$ could be responsible for compensating the surface of positively polarized films under high $p\rm O_2$ conditions. Negative charge carried by the oxygen is exerted to upper surface of PT film, which can compensate on the (0, 0, P_3) domain surface charges and result in the decrease of the depolarization energy. Therefore, the positive polarization is enhanced. On the contrary with the same stage, the negative charge can decrease the fraction of the domain with polarization (0, 0, $-P_3$). When the PT film is equilibrated at ultralow oxygen pressures, the polarization is in the inward.[9,10] For ultrathin film without a covering electrode layer, the single domain state is extremely unstable due to larger depolarization energy. In our simulation, we give the inward polarization distribution for the ultrathin film (Fig. 2(a)). When an oxygen atom located at $x_1=x_2=32$ nm and $x_3=5$ nm is absorbed into the surface of the thin film, the two negative charges are set free

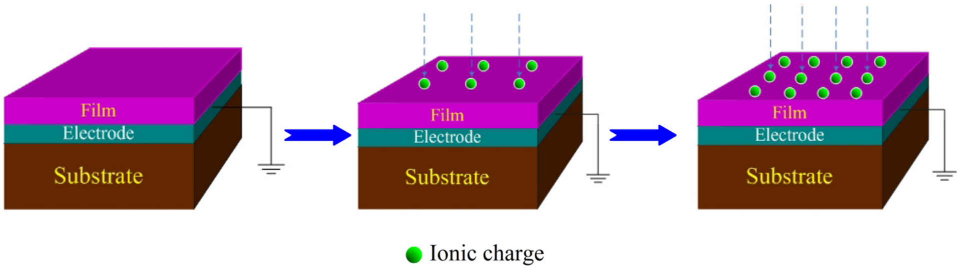

FIG. 1. (Color online) Diagram of the ferroelectric thin film at oxidizing atmosphere.

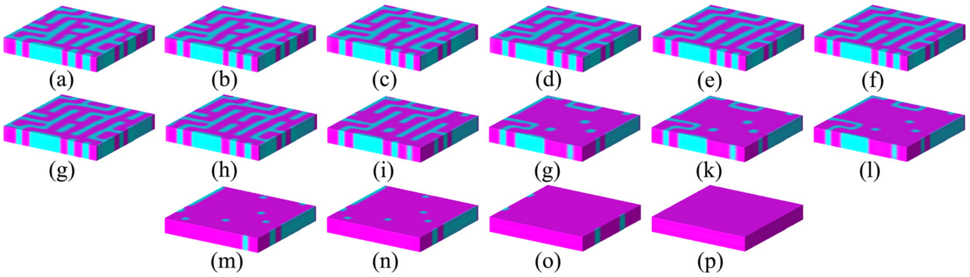

FIG. 3. (Color online) Domain evolution of the ferroelectric thin film, i.e., (a)-(p), controlled by the ionic charge density due to oxidizing atmosphere from 0.005 C/m^2 to 0.0425 C/m^2 with a interval 0.0025 C/m^2.

from oxygen. The polarization near the charges are switched, and the domain wall between (0, 0, P_3) and (0, 0, $-P_3$) are shifted toward (0, 0, $-P_3$) for minimizing the depolarization energy (Fig. 2(b)). Results of the nine oxygen atoms located at $31 \le (x_1, x_2) \le 33$, $x_3 = 5$ nm show the distribution of polarization around the center of the film has larger change than that of an oxygen atom (Fig. 2(c)). For multi-domain state, an oxygen atom has little influence on the domain morphology, and nine oxygen atoms can enlarge (0, 0, $-P_3$) domain around the ionic charges (Figs. 2(d) and 2(e)).

When the surface ionic charges are evenly distributed on the film surface, the evolution of the domain structures of the FTF was simulated with the surface ionic charges increasing from 0 C/m^2 to 0.0425 C/m^2 carried by oxygen. The initial domain structure is shown in Fig. 2(d), and then changes of domain morphologies with increasing of the surface ionic charge density are shown in Figs. 3(a)–3(p). Our results show that the chemical potential at the bare surface gives an analogous effect of applied voltage and can drive the domain wall movement with the continuous increase of oxygen ions density. More importantly, it can be seen that the domain morphology of the FTF changes from a multi-domain to a monodomain state as the surface ionic charge density is 0.0425 C/m^2 (Fig. 2(p)). Together with the change of domain structure, the mean spontaneous polarization $\langle P_3 \rangle = \frac{1}{V}\int |P_3| \mathrm{d}V$ of (0, 0, P_3) and (0, 0, $-P_3$) have been plotted in Fig. 4, respectively. The circle line in Fig. 4 shows that the (0, 0, $-P_3$) domain is entirely eliminated and the (0, 0, P_3) single domain structure is formed in the PT film as the ionic surface charges density reaching 0.0425 C/m^2. The square line in Fig. 4 plot the volume fractions of (0, 0, $-P_3$) domain versus the surface charge density and also shows that the (0, 0, $-P_3$) domain fraction falls down rapidly as the surface ionic charge density reaching about 0.025 C/m^2 and almost disappears as the surface ionic charge density reaching about 0.0375 C/m^2.

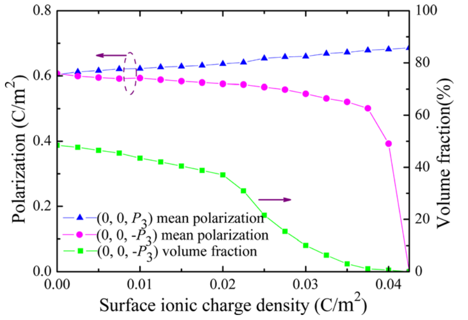

FIG. 4. (Color online) Mean polarizations of (0, 0, P_3) and (0, 0, $-P_3$) domain and the (0, 0, $-P_3$) domain volume fraction as a function of ionic surface charge density.

In summary, the changes of the domain structures of FTF with the surface ionic charges produced by the oxygen atmosphere were predicted. It is shown that oxidizing conditions favor a positive polarization directed towards the upper surface. The simulations demonstrate that the chemical potential can be used to control the domain patterns and magnitude of the spontaneous polarization, which can largely expand the applications of FTF, especially in chemical sensors.

This project is grateful for support from the NSFC (Nos. 10902128, 10732100, 10972239, 11072271, and 51172291), the Fundamental Research Funds for the Central Universities.

[1] A. N. Morozovska, S. V. Kalinin, E. A. Eliseev, V. Gopalan, and S. V. Svechnikov, Phys. Rev. B **78**, 125407 (2008).

[2] N. A. Pertsev and H. Kohlstedt, Phys. Rev. Lett. **98**, 257603 (2007).

[3] B. Wang, R. Xia, H. Fan, and C. H. Woo, J. Appl. Phys. **94**, 3384 (2003).

[4] Y. L. Li, S. Y. Hu, Z. K. Liu, and L. Q. Chen, Appl. Phys. Lett. **78**, 3878 (2001).

[5] J. Junquera and P. Ghosez, Nature **422**, 506 (2003).

[6] D. C. Ma, Y. Zheng, and C. H. Woo, Acta Mater. **57**, 4736 (2009).

[7] K. Garrity, A. M. Kolpak, S. Ismail-Beigi, and E. I. Altman, Adv. Mater. **22**, 2969 (2010).

[8] D. D. Fong, A. M. Kolpak, J. A. Eastman, S. K. Streiffer, P. H. Fuoss, G. B. Stephenson, Carol Thompson, D. M. Kim, K. J. Choi, C. B. Eom, I. Grinberg, and A. M. Rappe, Phys. Rev. Lett. **96**, 127601 (2006).

[9] R. V. Wang, D. D. Fong, F. Jiang, M. J. Highland, P. H. Fuoss, Carol Thompson, A. M. Kolpak, J. A. Eastman, S. K. Streiffer, A. M. Rappe, and G. B. Stephenson, Phys. Rev. Lett. **102**, 047601 (2009).

[10] J. Hlinka, Physics **2**, 8 (2009).

[11] Y. Kim, I. Vrejoiu, D. Hesse, and M. Alexe, Appl. Phys. Lett. **96**, 202902 (2010).

[12] J. Shin, V. B. Nascimento, G. Geneste, J. Rundgren, E. W. Plummer, B. Dkhil, S. V. Kalinin, and A. P. Baddorf, Nano Lett. **9**, 3720 (2009).

[13] M. J. Highland, T. T. Fister, M. I. Richard, D. D. Fong, P. H. Fuoss, C. Thompson, J. A. Eastman, S. K. Streiffer, and G. B. Stephenson, Phys. Rev. Lett. **105**, 167601 (2010).

[14] Y. L. Li, S. Y. Hu, Z. K. Liu, and L. Q. Chen, Appl. Phys. Lett. **81**, 427 (2002).

[15] Y. Zheng, B. Wang, and C. H. Woo, Phys. Lett. A **368**, 117 (2007).

[16] Y. Zheng and C. H. Woo, Appl. Phys. A **97**, 617 (2009); C. H. Woo and Y. Zheng, Appl. Phys. A **91**, 59 (2008).

[17] Y. Zheng, C. H. Woo, and B. Wang, Nano Lett. **8**, 3131 (2008).

[18] M. E. Lines and A. M. Glass, *Principles and Applications of Ferroelectrics and Related Materials* (Clarendon, Oxford, 1979).

[19] G. Rupprecht and B. O. Bell, Phys. Rev. **135**, A748 (1964).

[20] C. Kittel, *Introduction to Solid State Physics* (New York, John Wiley & Sons, 2005).

[21] D. C. Lupascu, *Fatigue in Ferroelectric Ceramics and Related Issues* (Berlin, Springer–Verlag, 2004).

[22] N. A. Pertsev, A. G. Zembilgotov, and A. K. Tagantsev, Phys. Rev. Lett. **80**, 1988 (1998).

[23] The list of the parameters of PT used in the calculations are $\alpha_1 = 3.8 \times (T - 752) \times 10^5$ C^{-2} m^2 N, $\alpha_{11} = -7.3 \times 10^7$ C^{-4} m^6 N, $\alpha_{12} = 7.5 \times 10^8$ C^{-4} m^6 N, $\alpha_{111} = 2.6 \times 10^8$ C^{-6} m^{10} N, $\alpha_{112} = 6.1 \times 10^8$ C^{-6} m^{10} N, $\alpha_{123} = -3.7 \times 10^9$ C^{-6} m^{10} N, $Q_{11} = 0.089$ C^{-2} m^4, $Q_{12} = -0.026$ C^{-2} m^4, $Q_{44} = 0.03375$ C^{-2} m^4, $s_{11} = 8.0 \times 10^{-12}$ m^2 N^{-1}, $s_{12} = -2.7 \times 10^{-12}$ m^2 N^{-1}, $s_{44} = 9.24 \times 10^{-12}$ m^2 N^{-1}, $\delta^{eff} \approx 2.8$ nm, $\varepsilon_b \approx 50\varepsilon_0$, $G_{1111} = 3.46 \times 10^{-10}$ C^{-2} m^4 N, $D_{11} = 3.46 \times 10^{-10}$ C^{-2} m^4 N, $D_{44} = 1.73 \times 10^{-10}$ C^{-2} m^4 N.

[24] L. Q. Chen, Phys. Ferroelectr. **105**, 363 (2007).